Mathematical modelling and simulation of an inclined solar water desalination unit.

Jakobus Myburgh[a], Fareed Ismail[b], Ouassini Nemraoui[c]

Abstract— A Mathematical model was developed to determine the efficiency of producing fresh water on a small scale when changing some parameters of an inclined solar water desalination unit. The object was to investigate the effect of changing various parameters such as the flow rate, irradiance and average temperature suitable for weather conditions in the Western Cape, Cape Town. The optimal water flow rate of 100 ml/min over a 1 m2 flat plate absorber was found suitable to achieve the maximum evaporation. The Solar irradiance was limited between 500 and 1000 W/m2. The ambient temperature was set at 28^0C, the wind factor was ignored at this stage. The steady state of the system was reached after an hour and the determination of fresh water production during 8 hours of daylight was found to be between 3.5 and 7.7 l/day respectively. The results found were in good agreement with experimental results in similar environment as Cape Town.

***Index Terms*—Solar Energy, Desalination, Mathematical Modelling, Inclined Solar Water Desalination.**

1 INTRODUCTION

There is a growing demand for potable water in all countries [1]. Fresh water resources are limited. The world's water resources consists 97.25% of seawater and 2.05 % of water resources unusable in ice caps and glaciers. The salt ground water and inland salt seas reduce the available fresh water even further. Less than 0.7 % of Earth's water is available as potable water [2]. The fresh water usage in South Africa is 29% Domestic, 6% Industrial and 59% Agricultural [3].

The South African Department of water and Sanitation set the minimum quantity of fresh water at 25 litres per person per day and the maximum cartage distance at 200 metres; 11% of the country lacks access to this minimum standard [4].

Desalination is the most widely used process to purify water in many countries. The conventional desalination processes Reverse Osmosis and Multi-Stage flash has high energy requirements that are usually supplied with non-renewable energy sources such as burning of fossil fuels [5]. These methods of desalination have high initial installation costs with high maintenance costs. The growing energy and water demand along with depletion of non-renewable resources shifted focus towards renewable energy solutions. Desalination using solar still requires minimal initial investment cost and would be sustainable process to convert salty water into fresh water [6], [7]. South Africa has a high level of solar radiation [8], [9]. Most areas in South Africa receive an average of 4.5 to 6.5 kWh/m^2 solar radiation on average per day [10], which could be used for solar desalination. A compact transportable solar desalination unit would be beneficial to remote areas where water piping network are limited.

An experimental study on an Inclined Solar Water Desalination System (ISWD) system with different absorber mediums showed that using a black wick material increased the overall production of fresh water compared to a black absorber plate. The water purity was also affected using different absorber mediums [11], [12]. A Mathematical model for an ISWD unit was developed which could predict the fresh water output under the climatic conditions of Cyprus. The model focuses on adjusting of the solar irradiance and feed rate of brackish water for the system [13].

Jones J investigated the effect of wind and cover material on the fresh water yield of a passive solar still. The research indicated that using a glass cover proved more effective than using plexiglass or plastic wrap [14], [15].

The aim of this paper was to develop and simulate a Mathematical Model of an ISWD System that could predict the output of fresh water in the Western Cape, Cape Town area. The effect of mass flow rate and temperature on the output of the system along with the heat transfer is explained.

2 DESCRIPTION OF SYSTEM

The Inclined Solar Water Desalination System (ISWD) shown in Fig. 1 is simulated to have the following parameters:

The insulated box is inclined at 30^0, box consists of an absorber plate (mild steel) painted matte black for maximum solar absorptivity, the cover is made of glass with a high Transmissivity, the box creates a sealed cavity where the height, width and length are 0.2m, 1m, and 1m. The System is insulated on all sides except the glass cover to reduce the thermal energy losses in the system. The feed water is supplied to the distribution pipe using gravity at an adjustable rate. The water distribution pipe has Ø 1mm holes along the pipe spaced 10mm apart to spray the water uniformly across the absorber plate. The water would form a thin layer (around 3mm) across the plate. The system is angled at 30^0 to allow the water to flow down the absorber plate and the solar rays would be 90^0 to the absorber plate at peak solar irradiance during daytime. Solar energy heats the system and some of the brackish water on the absorber plate gets evaporated. The heated evaporated water touches the relatively cool glass cover and condenses to droplets; then flows down the inclined glass cover into the fresh water

a. Jakobus Myburgh, Cape Peninsula University of Technology, PO Box 1906, Bellville 7535, South Africa (email: jjmybie@gmail.com)
b. Fareed Ismail, Cape Peninsula University of Technology, PO Box 1906, Bellville 7535, South Africa (email: ismailf@cput.ac.za)
c. Ouassine Nemraoui, Cape Peninsula University of Technology, PO Box 1906, Bellville 7535, South Africa (email: nemraouio@cput.ac.za)

collector pipe exiting the cavity. The remaining brackish flows down the absorber plate into a separate waste tank.

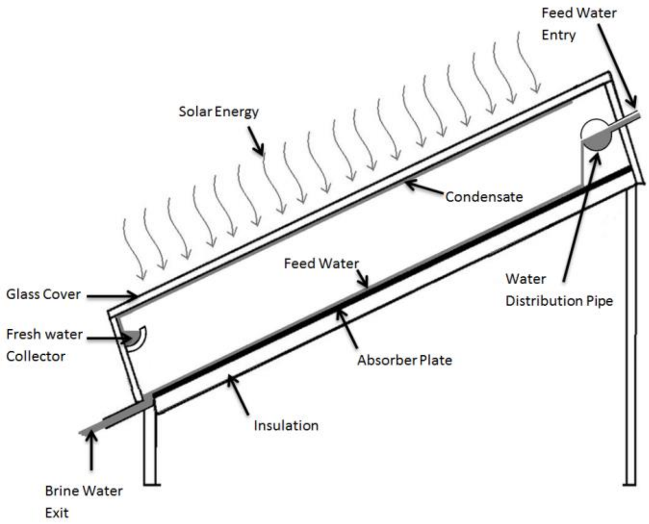

Fig. 1. Schematic of an Inclined Solar Water Desalination System

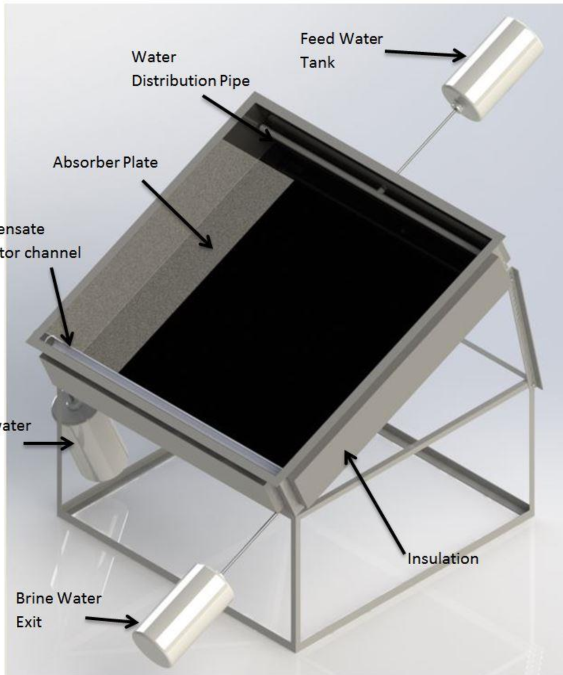

Fig. 2. Drawing of an Inclined Solar Water Desalination System

3 MATHEMATICAL MODELLING OF THE SYSTEM

A simulation model is developed to predict the thermal and mass flow performance of the ISWD system using the following assumptions:

i. The sun rays are aligned to the normal of the ISWD system.
ii. The system is insulated on all sides of the inclined box except the glass cover; it is assumed the energy loss from system to the outside walls is zero.
iii. The effect of wind speed on the convection heat transfer between the glass and the outside air is negligible.
iv. The water is distributed uniformly across the absorber plate.
v. All the condensate is collected from the cavity into the collector pipe.

Energy balances are performed at critical components in the ISWD system such as the absorber plate, water flowing on the absorber plate and the glass cover. Eq. (1) shows the energy balance equation for the absorber plate. Fig. 3 shows the thermal processes that are acting on the absorber plate.

$$\Delta E = M_p C_p \frac{dT_p}{dt} = Solar\ Radiation - Q_{r,p-g} - Q_{c,p-w} \tag{1}$$

The Solar Radiation is calculated as:

$$Solar\ Radiation = I\tau\alpha \tag{2}$$

M_p Is the mass of the absorber plate, $C_p$is the specific heat capacity of the absorber plate, T_p and is the temperature of the absorber plate. The total solar radiation is represented by I, τ is the Transmissivity of the glass and α is the absorptivity of the absorber plate. $Q_{r,p-g}$ represents the radiation heat transfer from the absorber plate to the glass cover and $Q_{c,p-w}$ is the convection heat transfer from the absorber plate to the water.

$$Q_{c,p-w} = h_{c,p-w}\,(T_p - T_w) \tag{3}$$

$$Q_{r,p-w} = h_{r,p-g}\,(T_p - T_w) \tag{4}$$

$h_{r,p-g}$ Is the Radiation heat transfer coefficient between the absorber plate and the glass cover and $h_{c,p-w}$ is the convection heat transfer coefficient between the absorber plate and the water flowing over the plate.

$$h_{r,p-g} = \varepsilon_p \sigma (T_p + T_g)({T_p}^2 - {T_g}^2) \tag{5}$$

σ Is the Stefan-Boltzmann constant σ=5.670367x10^{-8} W/m^2.K^{-4} and ε_p is the Emissivity of the absorber plate.
Eq. (2)-(5) is substituted into the energy balance equation for the absorber plate.

$$M_p C_p \frac{dT_p}{dt} = I\alpha\tau - h_{r,p-g}\,(T_p - T_g) - h_{c,p-w}\,(T_p - T_w) \tag{6}$$

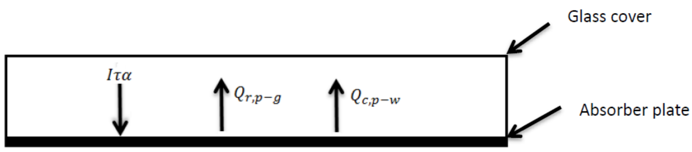

Fig. 3. Energy balance at the absorber plate.

Fig. 4 shows the heat balance equation at the water flowing in the system. The water flowing over the system is modelled as a single unit. The average temperature of the water flowing over the plate is calculated in Eq. (7).

$$\Delta E = p_w C_w b \frac{dT_{w,ex}}{dt} = C_w(\dot{m}_{in} T_{w,in} \text{-} \dot{m}_{ex} T_{w,ex})\frac{1}{L} + Q_{c,p-w} - Q_{evap} \tag{7}$$

p_w Represents the density of water, C_w the specific heat capacity of water, $\dot{m}_{in}$ the mass flow of water entering the system, $\dot{m}_{ex}$ is Mass flow of water exiting the system and b is the film thickness of the water. L is the length of the cavity.

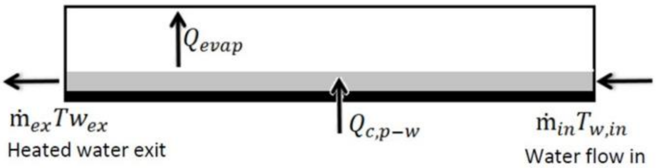

Fig. 4. Diagram for Energy balance at the water flowing over the absorber plate.

Eq. (8) is used to calculate the exit mass flow rate of the water.

$$\dot{m}_{ex} = \dot{m}_{in} - \dot{m}_{evap}L \tag{8}$$

Evaporation mass flow rate per m^2 is calculated in Eq. (9).

$$\dot{m}_{evap} = \frac{Q_{evap}}{h_{fg}} \tag{9}$$

h_{fg} Represents the Latent heat of evaporation. The energy equation for the glass cover:

$$\Delta E = M_g C_g \frac{dT_g}{dt} = Q_{r,p-g} + Q_{cond} - Q_{r,g-a} - Q_{c,g-a} \tag{10}$$

The M_g and C_g are the mass and the specific heat of the glass cover. $Q_{r,g-a}$ Represents the radiation heat flux between the glass cover and the ambient air. $Q_{c,g-a}$ Is the convention heat flux between the glass cover and the ambient air.

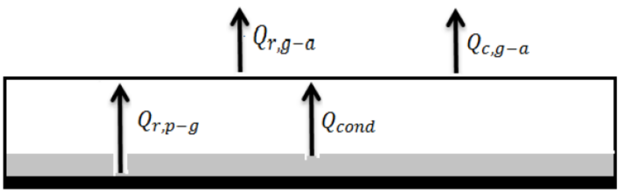

Fig. 5. Diagram for the energy balance at the glass cover.

$$Q_{r,g-a} = h_{r,g-a}\,(T_g - T_a) \tag{11}$$

$$Q_{c,g-a} = h_{c,g-a}\,(T_g - T_a) \tag{12}$$

Where $h_{r,g-a}$ is the Radiation Heat transfer coefficient from glass to air and $h_{c,g-a}$ is the Convection Heat transfer coefficient from glass to air.

$$\dot{m}_{cond} = \frac{Q_{cond}}{h_{fg}} \tag{13}$$

Where $\dot{m}_{cond}$ is the mass flow rate of water condensation. Q_{cond} Represents the condensation heat flux and h_{fg} is the latent heat of vaporization. The vapour mass balance equation:

$$\frac{dM_v}{dt} = \left(\dot{m}_{evap} - \dot{m}_{cond}\right)LW \tag{14}$$

Where M_v is the vapour mass within the cavity and W is the width of the cavity. The partial pressure of air and vapour can be calculated should the temperature of the vapour and air is known along with the mass of the air and vapour.

$$P_a = \frac{M_a R_a T_v}{V} \qquad P_v = \frac{M_v R_v T_v}{V} \qquad P = P_a + P_v \tag{15}$$

P_a Is the pressure of the air inside the cavity, P_v is the pressure of the air-vapour mixture inside the cavity T_v is the temperature of the air-vapour mixture inside the cavity and P is the total pressure inside the cavity. The saturation pressure is determined by using the equation of:

$$P_{sat} = P(T_m) \tag{15}$$

The Arden Buck empirical correlation [16] is used to calculate the saturation pressure for moist air using the temperature of the vapour air mixture.

$$P_{sat} = 0.61121 \exp(\left(18.678 - \frac{T}{234.5}\right) \ldots \left(\frac{T}{257.14+T}\right)) \times 1000 \tag{16}$$

For liquid water, T>0 ^{0}C

Where P_{sat} is the saturation pressure of steam. The relative humidity and specific humidity can be calculated from:

$$\omega = \frac{M_v}{M_a} \qquad H_R = \frac{P_v}{P_{sat}} \tag{17}$$

Where ω is the absolute humidity and H_R is the relative humidity. The energy lost by evaporation is determined by using the Ryan Correlation [17]. The correlation is based on investigations on open bodies of water such as lakes and ponds. The original correlation is made for wind velocities, which is adapted to exclude wind to give the Eq. (18).

$$Q_{evap} = 0.027(T_v - T_w)^{\frac{1}{3}} P_{sat}(1 - H_R) \tag{17}$$

Eq.(3) and (17) is substituted into the energy balance equation for water:

$$p_w C_w b \frac{dT_{w,ex}}{dt} = C_w(\dot{m}_{in}T_{w,in}\text{-}\dot{m}_{ex}T_{w,ex})\frac{1}{L} + h_{c,p-w}\,(T_p - T_w) - 0.027(T_v - T_w)^{\frac{1}{3}} P_{sat}(1 - H_R) \tag{18}$$

Evaporation heat flux between the air-vapour mixture is calculated using the Ryan correlation shown as:

$$Q_{cond} = 85.0(T_v - T_g)H_R \tag{19}$$

Substituting Eq.(4) and Eq.(19) into the energy balance equation of the glass cover:

$$M_g C_g \frac{dT_g}{dt} = h_{r,p-g}(T_p - T_g) + 85.0(T_v - T_g)H_R - h_{r,g-a}\,(T_g - T_a) - h_{c,g-a}\,(T_g - T_a) \tag{20}$$

4 Results with Discussion

The heat and mass transfer equations were simulated in Matlab. The equations are solved in iterations per second. The system is modelled per m^2 to allow for scaling of the system. The parameters used are listed in Table I. The system uses Empirical relationships to determine properties that change with system temperatures as the system functions. The temperature difference between the moist air and water flowing over the absorber plate was determined to be 2^0C by [11].

Table I: System Parameters

Symbol	Value	Unit	Description
M_p	7.95	kg/m^2	Mass of absorber plate
C_p	490	J/kg.K	Specific heat of absorber of absorber plate
ε_p	0.08	-	Emissivity of absorber plate
α	0.96	-	Absorptivity of absorber plate
M_g	7.6	kg	Mass of glass cover
ε_g	0.89	-	Emissivity of glass
τ	0.89	-	Transmissivity of glass
p_g	2600	kg/m^3	Density of glass
p_w	998	kg/m^3	Density of water
C_w	4184	J/kg.K	Specific heat of water
h_{fg}	2400×10^3	J/kg	Latent heat of evaporation
M_a	0.24	kg/m^2	Mass of air inside cavity
$h_{c,p-w}$	40	W/m^2.K	Convective heat transfer coefficient between plate and water
$h_{c,g-a}$	40	W/m^2.K	Convective heat transfer coefficient between glass and air

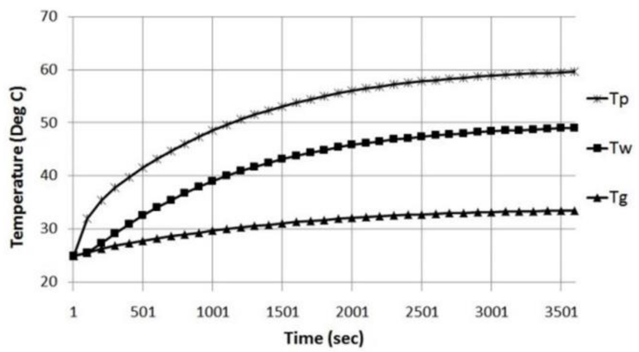

Fig. 6. The effect of changing the mass flow rate and solar irradiance on the temperatures of the absorber plate, the flowing water and the glass cover.

To determine the effect of solar intensity and mass flow rate on the System, some parameters where kept constant. The system is simulated using 500W/m^2 irradiance, ambient air temperature of 25^0C and a mass flow rate of 100ml/min (5.99kg/h). The simulation is run for one hour with an iteration being done every second. The initial temperature of all the system components is taken as 25^0C and the ambient air temperature is constant at 25^0C. The system reaches a steady state after one hour of operation. Fig. 6 shows the temperature change of the absorber plate (T_p), flowing water (T_w) and the glass cover (T_g) from a simulating the system for 1 hour.

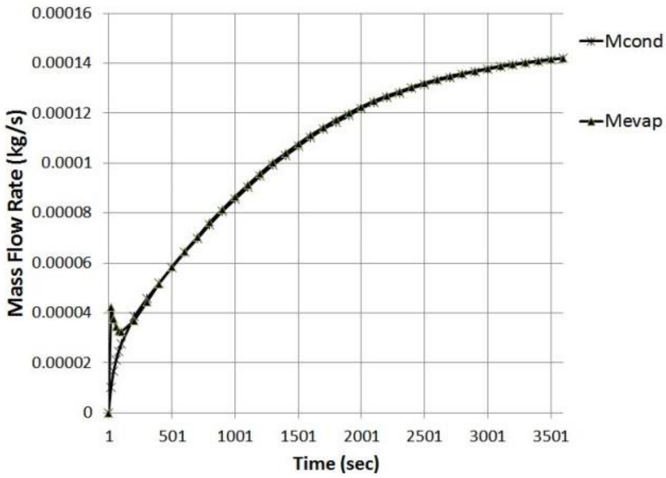

Fig. 7. Mass flow of evaporation and condensation in the system versus time.

The surge in the first 50 seconds in mass flow rate of evaporation from Fig. 7 is attributed to the cavity having zero humidity at the initial stage. The mass flow rate of evaporation and condensation splits in the first 50 seconds then equals out as the system approaches the steady state.

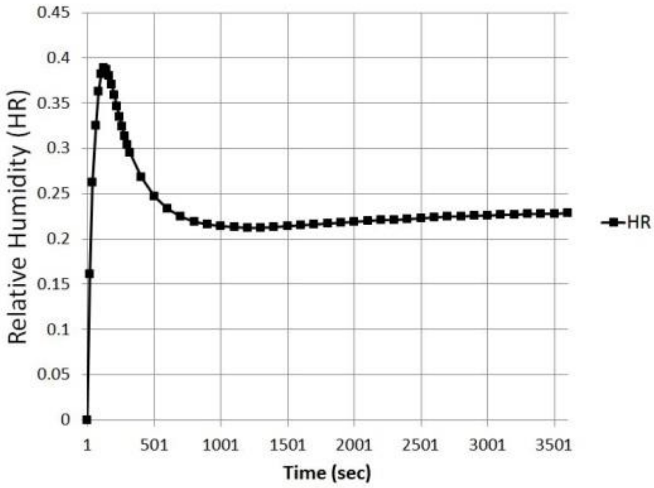

Fig. 8. Relative humidity of air vapour mix inside the cavity compared to time.

Table II: The effect of mass flow rate and solar irradiance on the output of an ISWD System

	50ml/min (2.99kg/h)	100ml/min (5.99 kg/h)	150ml/min (8.98 kg/h)
SI (W/m2)	M_{cond} (kg/h)	M_{cond} (kg/h)	M_{cond} (kg/h)
250	0.2619	0.2301	0.2077
500	0.5323	0.4425	0.38
750	0.8391	0.6899	0.5819
1000	1.164	0.9607	0.8082
1250	1.5003	1.2472	1.0524

The mass flow rate and the solar irradiance on the system are altered to investigate the effect on fresh water production and the results are indicated in Table II for the simulation run in Fig. 6. To calculate the fresh water production per hour the mass flow rate of condensation at the steady state is used over a period of one hour. The system would produce less than the indicated amount for the first hour while it heats to the steady state. Table II shows that the system produces more fresh water when the mass flow rate of feed water is decreased. Increasing the solar irradiance increases the output of fresh water.

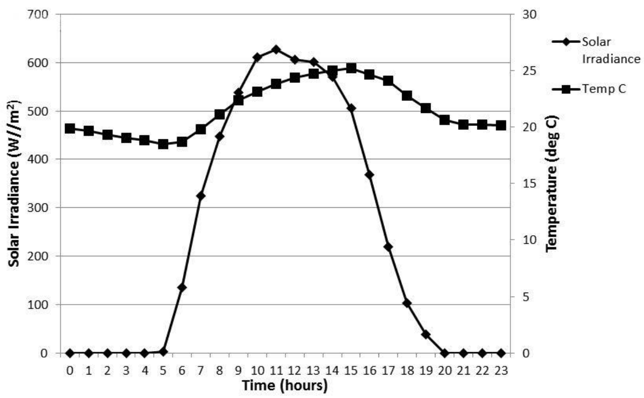

Fig. 9. Solar Irradiation and Temperature conditions in Cape Town for the average day in January 2018.

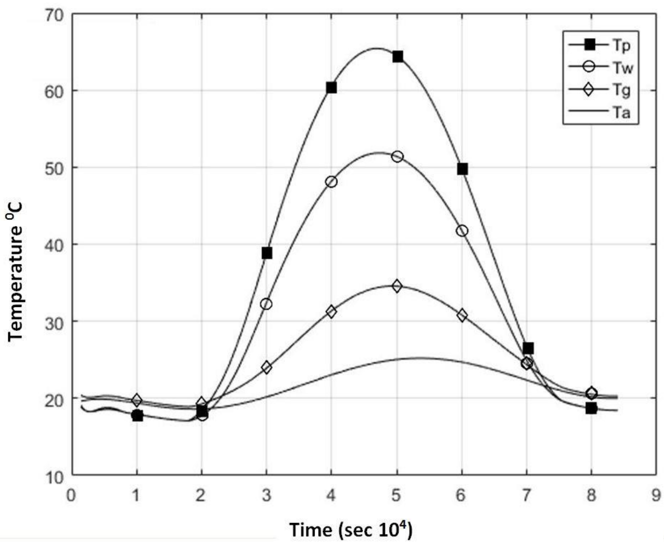

Fig. 10. Simulated temperatures for the time variable air temperatures and solar irradiance.

The model was developed to be able to simulate the production of fresh water from actual weather conditions where the solar irradiation and air temperature could be entered to the model in the form of a Polynomial Equation.

The solar irradiance and air temperature for an average day in Western Cape, Cape Town from January 2018 [18] is shown in Fig. 9. The solar irradiance and air temperatures are used by the simulation along with system parameters to predict the temperature changes of various components of the ISWD system as shown in Fig. 10.

5 CONCLUSION

The effect of mass flow rate of the feed water and temperature on the output of the system along with the heat transfer model is shown with results and explained. The system could produce between 3.54L and 7.69L of fresh water with 8 hours of solar irradiance of 500W/m^2 to 1000W/m^2 on average summer day in the Cape Town area.

Possible future work could include the testing of a prototype ISWD unit in the area. Solar tracking, heat loss to outside walls and wind effects on the system which have been excluded in this model could be implemented into the model to increase the accuracy of results from simulating the system.

REFERENCES

[1] UNESCO, Global Water Resources Under Increasing Pressure from Rapidly Growing Demands and Climate Change, According to New UN World Water Development Report, WWDR4—Background Information Brief, United Nations World Water Assessment Program, 2012, UNESCOPRESS

[2] Pidwirny, M. (2006). "The Hydrologic Cycle". Fundamentals of Physical Geography, 2nd Edition. [online], http://www.physicalgeography.net/fundamentals/8b.html

[3] No Author. (2015). Who is using all the water in South Africa?.[online], https://businesstech.co.za/news/general/104441/who-is-using-all-the-water-in-south-africa/ Accessed 28/05/2018

[4] Johnson, M. (2017).*Water & Sanitation: Statistics SA analysis; Water & Sanitation Infrastructure: Auditor-General performance audit meeting 24 January 2017*. Water & Sanitation. Parliament of South Africa, Cape Town

[5] Shatat, M. and Riffat, S.B., 2012. Water desalination technologies utilizing conventional and renewable energy sources. International Journal of Low-Carbon Technologies, 9(1), pp.1-19.

[6] Ranjan, K.R. and Kaushik, S.C., 2013. Economic feasibility evaluation of solar distillation systems based on the equivalent cost of environmental degradation and high-grade energy savings. International Journal of Low-Carbon Technologies, 11(1), pp.8-15.

[7] Manokar, A.M., Winston, D.P., Kabeel, A.E. and Sathyamurthy, R., 2018. Sustainable fresh water and power production by integrating PV panel in inclined solar still. Journal of Cleaner Production, 172, pp.2711-2719.

[8] Singh, J., 2016. Ranking South African provinces on the basis of MERRA 2D surface incident shortwave flux. Journal of Energy in Southern Africa, 27(3), pp.50-57.

[9] Sebitosi, A.B. and Pillay, P., 2008. Renewable energy and the environment in South Africa: A way forward. Energy policy, 36(9), pp.3312-3316.

[10] South African Department of Energy. solar-power.[online], http://www.energy.gov.za/files/esources/renewables/r_solar.html Accessed 28/05/2018

[11] Aybar, H.Ş., Egelioğlu, F. and Atikol, U., 2005. An experimental study on an inclined solar water distillation system. Desalination, 180(1-3), pp.285-289.

[12] Ahmed, H.M., 2016, August. The effects of various types and layouts of wick materials on the thermal performance of conventional solar stills. In Smart Energy Grid Engineering (SEGE), 2016 IEEE (pp. 84-89). IEEE.

[13] Aybar, H.Ş., 2006. Mathematical modeling of an inclined solar water distillation system. Desalination, 190(1-3), pp.63-70.

[14] J. Andrew Jones, Laura W. Lackey & Kevin E. Lindsay (2013) Effects of wind and choice of cover material on the yield of a passive solar still, Desalination and Water Treatment, 52:1-3, 48-56, DOI: 10.1080/19443994.2013.784715

[15] Zuo, L., Zheng, Y., Li, Z. and Sha, Y., 2012. Experimental investigation on the effect of cover material on the performance of solar still.

[16] Buck, A. L. (1981), "New equations for computing vapor pressure and enhancement factor", J. Appl. Meteorol., 20: 1527–1532

[17] Yilmaz, T.P. and Aybar, H.S., 1999. Evaluation of the correlations for predicting evaporative loss from water body. ASHRAE Transactions, 105, p.185-190.
[18] Local Weather Table View. Meteo Cape Town (2018).[online], http://www.meteo.capetown/pages/station/climate.php?var=T Accessed 28/05/2018

AUTHORS

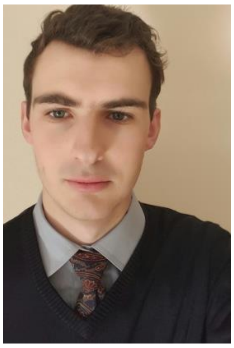

Jakobus Johannes Myburgh obtained his BTech Degree in Mechanical Engineering in 2017 from the Cape Peninsula University of Technology. He is currently doing his Master's Degree in Mechanical Engineering at the Cape Peninsula University of Technology.

Fareed Ismail obtained his Master's Degree in Mechanical Engineering in 2013 from the Cape Peninsula University of Technology (CPUT). He is an academic at CPUT with 16 years naval engineering design experience. He is a key figure in a community outreach programme; using his Doctoral research, he implemented a project that spans beyond the confines of academia, by expanding the field of multidisciplinary knowledge in the areas of engineering, design, renewable energy, marine life and agriculture, thus enriching the lives of children in a needy community in the Western Cape region of South Africa. Fareed has received the CPUT Outstanding Community Engagement Award in 2015 and his community project won the South African Provincial and National Early Childhood Development Programme Awards (2015). He is also the inventor and patent holder for the Modular Aquaponics Assembly.

Ouassini Nemraoui holds a PhD from the University of Paris Sud in the field of materials sciences. His research is in the field of advanced and multifunctional nano-materials for applications in energy conversion and management. He is an expert in the field of vacuum technology, thin films and nano-composites synthesis and optoelectronic devices.

Presenting author: The paper will be presented by Jakobus Johannes Myburgh.